JOURNAL OF BAKU ENGINEERING UNIVERSITY-ADVANCES IN CHEMISTRY AND CHEMICAL ENGINEERING
2024. Volume 8, Number 1 ***Pages 3-12***

UOT: 631.52:576.3
https://doi.org/10.30546/2521-6317.2024.205

MOLECULAR SIMULATION OF GEMINI-LIKE SURFACTANT BASED ON PROPOXYLATED ETHYL PIPERAZINE AND STEARIC ACID

Elgun E. HASANOV[1,2*], Ravan A. RAHIMOV[1,2]

[1]*Department of Chemical Engineering,*
Baku Engineering University, Hasan Aliyev str. 120,
Baku, Absheron, AZ0101, Azerbaijan
[2]*Institute of Petrochemical Processes of the Ministry of Science and Education of Azerbaijan,*
Hojaly ave. 30, AZ 1025, Baku, Azerbaijan

ARTICLE INFO

Article history:
Received 2024-08-11
Received in revised form:2024-09-20
Accepted:2024-10-15
Available online

Keywords:
Gemini-like;
Molecular simulation;
Ethyl piperazine;
DPD;
Stearic acid

ABSTRACT

Molecular simulation of a gemini-like surfactant 1-(propane-2-olyl)-4-ethylpiperazine-1,4-di-ium di-octadecanoate is performed applying Dissipative Particle Dynamics (DPD) methodology. Coarse graining of the surfactant and water molecules is done employing a well-established approach. The Flory-Huggins chi parameters were used for DPD parametrization. DPD simulation successfully predicts aggregation behavior of the surfactant solutions. Radial Distribution Function (RDF) curves of the gemini-like surfactant at varying concentrations are analyzed to determine orderly arrangements of molecules within solution. Existence of a second RDF peak at intermolecular distance range is related to the formation of aggregates. RDF curves approach to zero at higher distances due to very low concentration of molecules outside the aggregates. Critical Micelle Concentration (CMC) is calculated from DPD simulation outcomes and compared to the experimentally determined CMC value. Fluctuation of theoretically calculated CMCs at different concentrations is small and within acceptable limits. Even though the average theoretical CMC is greater than the experimental CMC value, both are in the same order of magnitude.

* Corresponding author.
E-mail addresses: ehasanov1@beu.edu.az (Elgun E. Hasanov).

1. Introduction

Surface-active compounds or surfactants are crucial components of various chemical products ranging from detergents to industrial drilling fluids. Due to their wide range of applications in science and technology and important place in day-to-day life of humans, surfactants and surface activity phenomena have been subject to in-depth scientific research. Computational chemistry is one of the most modern research methods being applied to investigate surface-active compounds. A suitable computational scheme for modelling and studying medium to large molecular systems including surfactant systems is Molecular Mechanics methods [1]. One of the most widely applied coarse-grained Molecular Mechanics tools standing out for its effectiveness and efficiency in modelling the behavior of surface-active compounds is called Dissipative Particle Dynamics (DPD) [2].

Recently several studies dedicated to DPD molecular simulations of various surfactant systems have been conducted. Vishnyakov et al. [3] applied DPD methodology for studying micellization behavior of non-ionic surfactants C_8E_8 (octaethylene glycol monooctyl ether $nC_8H_{17}(OCH_2CH_2)_8OH$), DDAO (dodecyldimethylamineoxide $nC_{12}H_{25}NO(CH_3)_2$) and MEGA-10 (N-decanoyl-N-methyl-D-glucamine $nC_9H_{19}(NCH_3)$ $(HCOH)_4CH_2OH$). They used a new approach of calculating DPD soft repulsion parameters utilizing infinite dilution activity coefficient data of the reference compounds. The authors confirmed that theoretically calculated CMC values from DPD simulations are closely matching the experimental CMC values of the investigated non-ionic surfactants. Gong et al. [4] used DPD simulation to investigate aggregation properties of quaternary ammonium surfactant hexyldimethyloctylammonium bromide (C_6C_8Br) in aqueous environment. They used angle evolution data extracted from DPD simulation to determine the configuration of C_6C_8Br molecules at different concentrations. It was established that as the surfactant concentration increases, the interior angle between alkyl chains of the surfactant becomes larger, thus the molecular configuration approaches a straight line. The authors related the experimental evidence of breakage of vesicle structure at higher concentrations to the formation of rigid linear structure of the C_6C_8Br molecules as revealed by DPD simulations. Goodarzi and Zendehboudi [5] employed DPD methodology to predict the interfacial behavior of water-oil emulsion in the presence of an inorganic salt and non-ionic surfactant hexaethyleneglycol monododecyl ether. They determined that increasing water/oil ratio in the simulation box resulted in interfacial tension to drop. Radius of gyration of surfactant molecules at the oil-water interface increased upon increasing the system temperature, indicating stretching of the molecules at the interface and thus reduction of interfacial tension. When an inorganic salt was introduced to the system, the interfacial tension initially dropped considerably due to the released ions shielding the repulsion between the surfactant headgroups at the interface. However, raising the salt concentration further did not result any visible change in interfacial tension, since the surfactant molecules saturated the interface. The authors verified the results deduced from the DPD simulation with previous experimental and theoretical works.

In this work we used DPD simulation to investigate micellization properties of a gemini-like surfactant 1-(propane-2-olyl)-4-ethylpiperazine-1,4-di-ium di-octadecanoate (C_{18}-EPPO-C_{18}) constructed from propoxylated ethyl piperazine and stearic acid. Theoretically evaluated parameters related to surfactant-water system were analyzed to determine the connection

between the molecular simulation and experimental properties of the surfactant. Synthesis and experimental measurements related to C_{18}-EPPO-C_{18} was done in one of our previous works [6].

2. Simulation Methods

2.1 DPD Theory

In DPD computation process Newton's classical laws of motion equations are solved for mesomolecular particles called beads to determine their final position and momenta and as a result to display the equilibrated configuration of the system [7] [8].

In molecular simulations the forces acting on a bead particle are categorized into non-bonded interaction forces and bonded interaction forces. The total sum of the forces due to non-bonded interactions is expressed via Eq. (1) below:

$$F_i = \sum_{i \neq j \neq k} F_{ij}^C + F_{ij}^D + F_{ij}^R + F_{ij}^E \quad (1)$$

Where F_{ij}^C is the conservative force, F_{ij}^D is the dissipative force, F_{ij}^R is the random force, and F_{ij}^E is the electrostatic force.

The conservative force F_{ij}^C expresses the repulsive interactions between two different bead particles. It simulates the specific chemical and physical characteristics of the molecules. For the current work the soft harmonic form of conservative force as expressed by Eq. (2) was used:

$$F_{ij}^C = \begin{cases} a_{ij}\left(1 - \frac{r_{ij}}{r_C}\right) & r_{ij} < r_C \\ 0 & r_{ij} \geq r_C \end{cases} \quad (2)$$

Where a_{ij} is called the interaction parameter between bead i and bead j, r_C is called the cut-off radius and r_{ij} expresses the distance between bead i and bead j.

The dissipative force F_{ij}^D expresses the frictional forces between the beads and is directly proportional to the approaching velocity of two beads. The dissipative force F_{ij}^D is expressed by Eq. (3) below:

$$F_{ij}^D = -\gamma_{ij}\omega^D(r_{ij})(v_{ij}) \quad (3)$$

Where γ_{ij} is called the friction coefficient and $\gamma_{ij} = \gamma_{ji} > 0$. $v_{ij} = v_i - v_j$ is difference between the velocities of two bead particles. ω^D is called distance dependent weight function and is calculated by Eq. (4) below:

$$\omega^D = \begin{cases} \left(1 - \frac{r_{ij}}{r_C}\right)^2 & r_{ij} < r_C \\ 0 & r_{ij} \geq r_C \end{cases} \quad (4)$$

The random force F_{ij}^R is included to simulate the effect of random motion of the beads in the liquid phase. It was calculated using the Eq. (5) below:

$$F_{ij}^R = \sigma_{ij}\omega^R(r_{ij})\xi_{ij}\frac{1}{\sqrt{\Delta t}} \quad (5)$$

Where σ_{ij} is called the noise amplitude and $\sigma_{ij} = \sigma_{ji} > 0$ holds true. ω^R is called distance dependent weight function, $\xi_{ij} = \xi_{ji} > 0$ is called randomly fluctuating Gaussian variable having a zero mean and a unit variance, Δt is the time step utilized when solving the DPD

equations. The distance dependent weight function ω^R is calculated via the Eq. (6) below:

$$\omega^R = \begin{cases} 1 - \frac{r_{ij}}{r_C} \; r_{ij} < r_C \\ 0 \; r_{ij} \geq r_C \end{cases} \tag{6}$$

The noise amplitude σ_{ij} in Eq. (5) is related to the friction coefficient γ_{ij} in Eq. (3) via the Eq. (7) below:

$$\sigma_{ij}^2 = 2\gamma_{ij} k_B T \tag{7}$$

Where k_B is the Boltzmann constant (k_B=*1.380649×10⁻²³ J·K⁻¹*) and T is the absolute temperature in units of *K*.

The electrostatic force F_{ij}^E was calculated according to Coulomb's Law as expressed by Eq. (8) below:

$$F_{ij}^E = k_e \frac{q_i q_j}{\varepsilon_r r_{ij}^2} \tag{8}$$

Where k_e is the Coulomb's constant (k_e=*8.99 × 10⁹ N · m² · C⁻²*), q_i and q_j are the electrostatic charges of the bead i and bead j, ε_r is the relative permittivity of the medium.

DPD forces related to bonded interactions are called spring force F_{ij}^S and angle force F_{ijk}^A. The spring force F_{ij}^S simulates the strength of bonds between bead particles and is expressed with the Eq. (9) and Eq. (10) below:

$$F_{ij}^S = -\frac{\delta U^S}{\delta r_{ij}} \tag{9}$$

$$U^S = \sum_j \frac{1}{2} C^b \left(r_{ij} - r_0\right)^2 \tag{10}$$

Where C^b is called the spring constant, r_0 is unstretched bond length between bead particles i and j.

The angle force F_{ijk}^A simulates the stiffness of the angle between two neighboring bonds and calculated using the Eq. (11) and Eq. (12) below:

$$F_{ijk}^A = -\frac{\delta U^A}{\delta r_{ij}} \tag{11}$$

$$U^A = \sum_j \frac{1}{2} C^a \left(cos\theta_{ijk} - cos\theta_0\right)^2 \tag{12}$$

Where C^a is called the angle constant, θ_{ijk} is the actual bond angle, θ_0 is the equilibrium bond angle of *i-j-k* bonds.

2.2 Coarse Graining

Coarse graining is done to transform the actual molecular structure of the component to a mesomolecular structure consisting of bead particles that is suitable for DPD simulation. Coarse graining of the gemini-like surfactant C_{18}-EPPO-C_{18} was done by dissecting the molecule into molecular fragments consisting of 4 or 5 heavy atoms. The dissection was done in a manner to keep the volumes of dissected parts approximately equal or close to each other. Coarse graining of the water molecules was done by combining 3 water molecules into a single bead particle. Coarse graining scheme for C_{18}-EPPO-C_{18} and water molecules is presented in Fig. 1 below.

Volume of a single water molecule is generally taken to be equal to 30 Å^3 in accordance with Groot and Rabone [9]. The total volume of W bead which contains 3 water molecules is generally considered to be 90 Å^3. Bead density of ρ=3 was adopted in-line with a pioneering work on DPD methodology by Groot and Warren [10]. The effective diameter of the beads was taken as equal to the bead interaction cut-off radius r_C and was determined using the Eq. (13) below [9]:

$$r_c = \sqrt[3]{\rho V_W} \tag{13}$$

Where V_W is bead volume of 90 Å^3. Therefore, the effective bead diameter for all beads becomes r_C=6.46 Å.

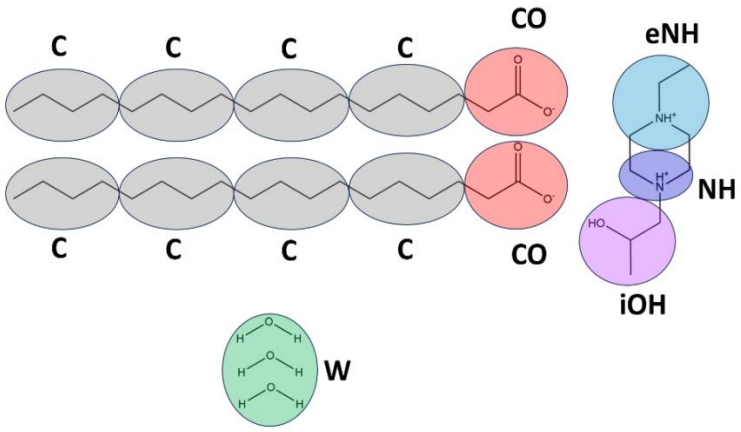

Fig. 1 Coarse graining of C_{18}-EPPO-C_{18} and water molecules

2.3 DPD Parametrization

The conservative force repulsive interaction parameters a_{ij} for the beads shown in Fig. 1 are calculated using the Flory-Huggins solution theory. The Flory-Huggins chi (χ_{ij}) parameter is related to DPD interaction parameter a_{ij} via the Eq. (14) below [9]:

$$a_{ij} = a_{ii} + \frac{\chi_{ij}}{0.231} \tag{14}$$

Where a_{ii} is the DPD interaction parameter between two identical beads, while a_{ij} is the interaction parameter for two differing beads. The Flory-Huggins chi (χ_{ij}) parameters for all bead pairs were calculated in Materials Studio v23 software. a_{ii} is calculated using the Eq. (15) below [9]:

$$a_{ii} = \frac{(16N_m - 1)k_B T}{0.2\rho} \tag{15}$$

Where N_m is the number water of water molecules combined into a single bead and ρ is the bead density. The values of bead interactions parameters a_{ii} and a_{ij} for all bead pairs are listed in Table 1 below.

The friction coefficient γ_{ij} from Eq. (3) above is assigned the value of γ_{ij}=4.5 as recommended by different works on DPD simulations of surfactants [5] [11] [12].

A time step of Δt=0.05 was selected to get good accuracy with optimum computational efficiency.

NH, eNH and CO beads were assigned electrostatic charges of +1, +1 and -1 respectively, while all other beads were electroneutral. The relative permittivity ε_r was set to the value of 78.2, which is the relative permittivity of water at 25°C to simulate the aqueous environment.

The value of spring constant in Eq. (10) was set to $C^b=150$ in-line with recommended value in the literature [12]. The unstretched bond length r_0 for all bead pairs was calculated using the Eq. (16) below [12]:

$$r_0 = r_C[0.1(n_i + n_j) - 0.01] \tag{16}$$

Where n_i and n_j are the number of heavy atoms contained by bonded beads i and j, respectively and r_0 is in units of Å.

The value of angle constant in Eq. (12) was set to $C^a=5$ and equilibrium angle of $\theta_0=180°$ was selected for all bond angles [12].

Table 1. Bead interaction parameters

Bead type	Reference compound	C	CO	iOH	NH	eNH	W
C	C_4H_{10}	78.33					
CO	CH_3COOH	134.22	78.33				
iOH	CH_3CHCH_3OH	89.25	93.35	78.33			
NH	CH_3NHCH_3	82.32	80.68	73.97	78.33		
eNH	$CH_3NCH_3CH_2CH_3$	79.38	77.98	74.75	78.18	78.33	
W	$3 \cdot H_2O$	118.79	80.77	75.50	74.24	72.69	78.33

3. Simulation Results

DPD simulations were run in a simulation box with dimensions of 200 Å × 200 Å × 200 Å at 2 mM, 5 mM, 10 mM and 20 mM surfactant concentrations for 100 000 time steps to reach equilibrated thermodynamic state. The thermostat was set to 298 K at the beginning of each simulation and box dimensions were fixed. All simulations were run in Materials Studio v23.

3.1 Micelle formation

DPD simulations could successfully predict micelle formation at various surfactant concentrations. The snapshots of final system configurations are presented in Fig. 2 below. Water beads have been hidden for clarity. The bead coloring scheme is the same as described in Fig. 1 above.

Fig. 2 indicates that the size and number of the aggregates increases as the concentration becomes greater. In addition, all CO beads, which simulate the polar part of the surface-active molecules, are directed away from the center of the aggregates and are in interaction with the solvent molecules. Certain fraction of the bead particles simulating the counterions with piperazine fragment are also interacting with the aggregates and forming a corona around them. The remaining counterion particles are freely distributed throughout the solution. The overall configuration of mesomolecules within the equilibrated simulation boxes agrees with the actual idea of the micelle formation and counterion binding to the micelles. This indicates that DPD parametrization is done correctly.

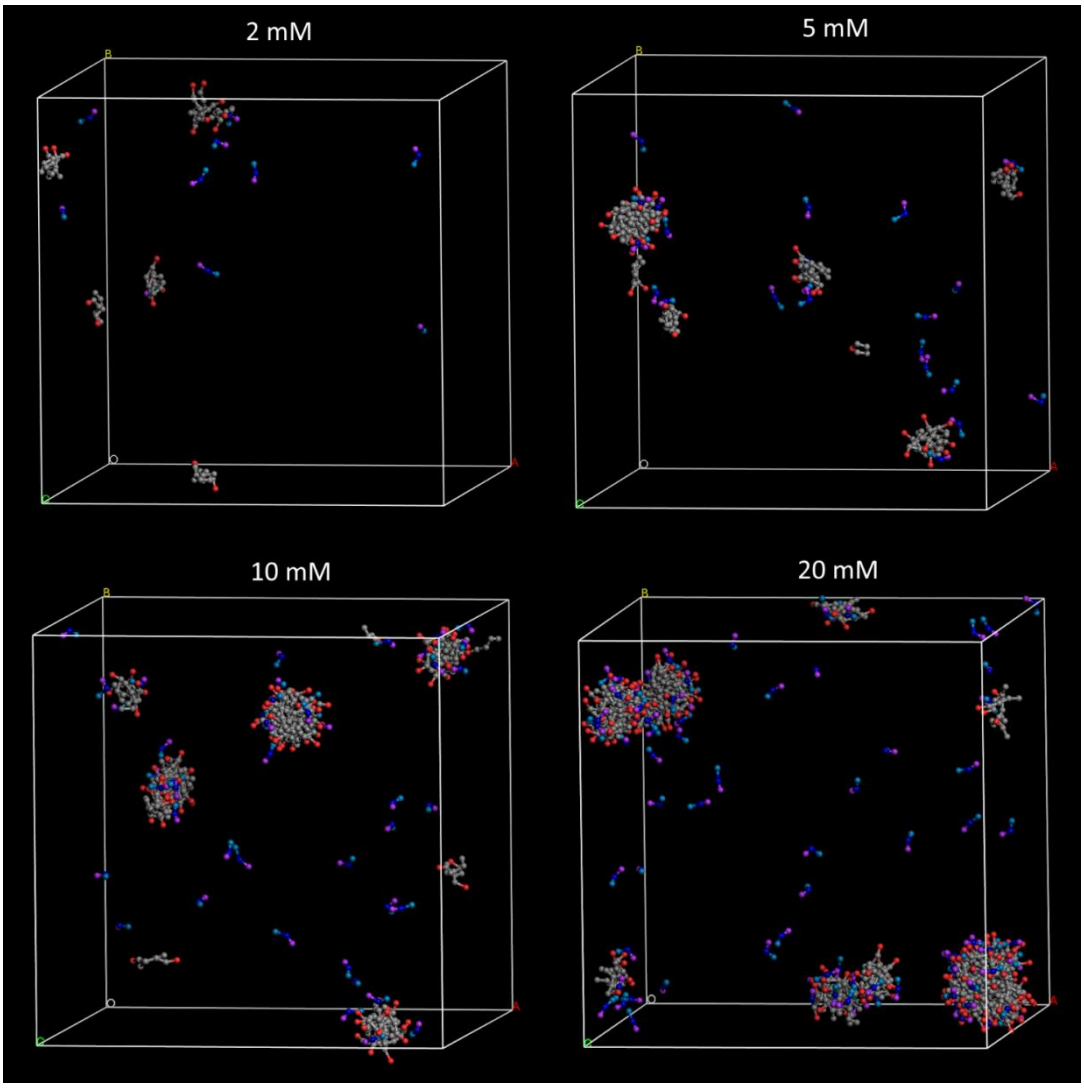

Fig. 2 Snapshots of equilibrated DPD simulation boxes at different concentrations

3.2 Radial Distribution Function (RDF)

Radial distribution function (RDF) describes how local density of the particles varies as a function of radial distance from the reference particle in a multiparticle system. When RDF curves are plotted for a multiparticle system it describes the averaged particle density calculated for each one of the particles over all distances. If a peak appears on an RDF plot at a certain radial distance, this is an indication of an orderly arrangement of the particles at this average distance from each other. RDF plots of C_{18}-EPPO-C_{18} are generated from the analysis of DPD trajectories to identify the structural arrangements of surface-active molecules within the solution space and presented in Fig. 3 below. The data has been normalized to compare the plots for varying concentrations.

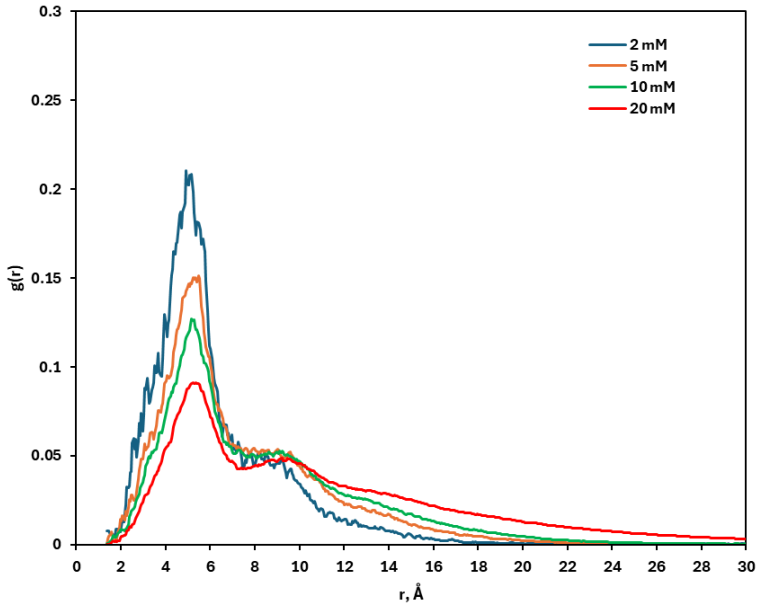

Fig. 3 RDF plots of C_{18}-EPPO-C_{18} at different concentrations

The analysis of Fig. 3 shows that the first RDF peak appears between 5-6 Å at all concentrations. This distance corresponds to the average equilibrium length of the bonds between bead particles. The height of the first peaks becomes smaller as the bulk surfactant concentration increases. A second, much flatter peak appears to the right of the first sharp peak on each one of the RDF curves for different concentrations. The height of the second peak becomes greater as the concentration is increased. While the first RDF peak is related to the intramolecular arrangement of beads, appearance of the second peaks is related to the ordered arrangement beyond the bond length distances. It could be argued that the second peak appears due to formation of the aggregates in the solution. The fact that the second peak becomes greater as the concentration increases supports this statement. The RDF curves decay and approach to zero as the distance increases. It is due to the fact that surface-active molecules are essentially concentrated within aggregates and probability of finding a surfactant molecule within interaggregate space is very low. This fact once more confirms the formation of micellar aggregates in the surfactant solution.

3.3 Prediction of CMC

CMC of a surfactant solution can be evaluated based on DPD trajectory analysis by identifying what fraction of the total dissolved surfactant molecules are freely distributed within the solution and are not part of any aggregates. The concentration of the 'free' surfactant molecules is counted as CMC. If two surfactant molecules are within a certain R_{agg} threshold distance from each other, they are considered to belong to the same aggregate. If the distance between two surfactant molecules is greater than R_{agg}, they are considered to be free from aggregates. R_{agg} is determined from the minimum point between the two peaks on the RDF curve (see Fig. 3). In addition, a cluster of surfactant molecules is considered as micelle if and only if it contains more than n_{mic} number of molecules. If less than n_{mic} number of molecules are in a cluster, all molecules are considered free from micellization. n_{mic} corresponds to the minimum point between two peaks on an aggregate size distribution curve. Aggregate size distribution curves of C_{18}-EPPO-C_{18} at varying concentrations are presented in Fig. 4 below.

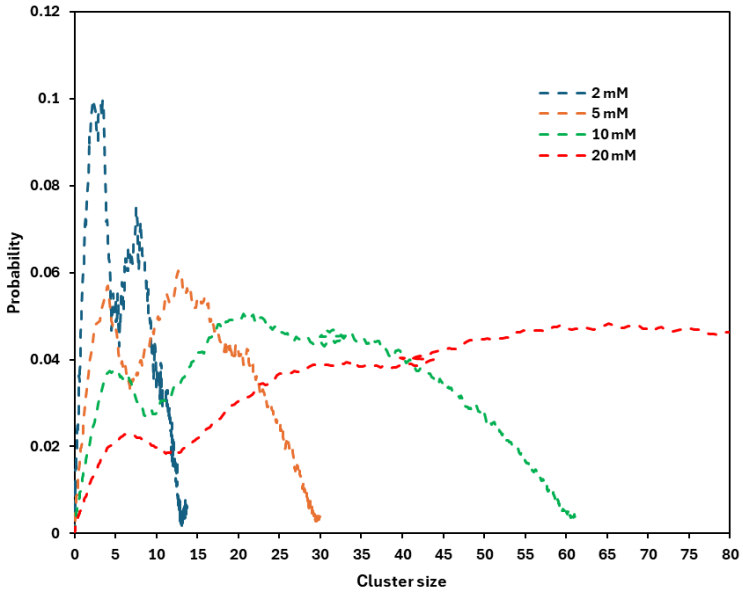

Fig. 4 Aggregate size distribution curves of C_{18}-EPPO-C_{18} at different concentrations

It is obvious from Fig. 4 that n_{mic} shows some variation with concentration. The value of n_{mic} is n_{mic}*=5, n_{mic}=7, n_{mic}=9 and n_{mic}=12* at 2 mM, 5 mM, 10 mM, and 20 mM concentrations, respectively. Theoretically evaluated CMC value was 1.054 mM, 1.157 mM, 1.398 mM and 0.681 mM for 2 mM, 5 mM, 10 mM, and 20 mM total concentrations, respectively. This level of fluctuation of CMC value with concentration can be considered normal. The average value of theoretical CMC was 1.073 mM whereas experimentally determined CMC value of C_{18}-EPPO-C_{18} is 0.390 mM [6]. In fact, several other studies reported a difference between experimental and theoretical CMC values of surfactants. Vishnyakov et al. [3] predicted the CMC values of non-ionic surfactants C_8E_8, DDAO and MEGA-10 as 11.8 mM, 1.3 mM, and 7.5 mM, respectively. The experimental CMC values of these surfactants are 10 mM, 1-2 mM, and 6-7 mM. Anderson et al. [11] predicted the CMC values of ionic n-alkyl sulfate surfactants S6S, S8S, S10S and S12S as 210 mM, 78 mM, 22.5 mM, and 6.7 mM, whereas their experimental CMC values were 420 mM, 130 mM, 33 mM, and 8.2 mM, respectively. Overall, theoretical and experimental CMC values of C_{18}-EPPO-C_{18} are in the same order of magnitude, which can be considered a very good agreement between simulation and experiment.

4. Conclusion

DPD simulation of a gemini-like surfactant C_{18}-EPPO-C_{18} constructed from propoxylated ethyl piperazine and stearic acid has been performed to model its micellization behavior. Repulsive interaction parameters have been evaluated utilizing the Flory-Huggins chi parameters. Simulations performed at different surfactant concentrations successfully predicted aggregate formation and its dependence on concentration. Aggregate formation has been verified from the analysis of RDF plots having a secondary peak at intermolecular range. The RDF curves are decaying and approaching zero at long distances, which points out that local concentration of surface-active molecules is very low outside the aggregate space. The average theoretically evaluated CMC value of C_{18}-EPPO-C_{18} was higher than experimental CMC value. However, the difference between theoretical and experimental CMC values is small and good agreement of simulation results with experimental outcomes is observed.

5. REFERENCES

[1] Ivanova, A. A., Koltsov, I. N., Groman, A. A., & Cheremisin, A. N. (2023). Molecular Dynamics Simulations for Surfactant Research (A Review). *Petroleum Chemistry*, *63*(8), 867–885. https://doi.org/10.1134/S0965544123060142

[2] Santo, K. P., & Neimark, A. V. (2021). Dissipative particle dynamics simulations in colloid and Interface science: a review. *Advances in Colloid and Interface Science*, *298*(October), 102545. https://doi.org/10.1016/j.cis.2021.102545

[3] Vishnyakov, A., Lee, M. T., & Neimark, A. V. (2013). Prediction of the critical micelle concentration of nonionic surfactants by dissipative particle dynamics simulations. *Journal of Physical Chemistry Letters*, *4*(5), 797–802. https://doi.org/10.1021/jz400066k

[4] Gong, J., Song, Y., Sun, Y., Sun, Q., Liu, C., Tan, J., Zhao, L., & Xu, B. (2024). Vesicle-to-micelle transition in a double chain quaternary ammonium surfactant system: Interfacial behavior and molecular insights. *Journal of Molecular Liquids*, *394*(August 2023), 123714. https://doi.org/10.1016/j.molliq.2023.123714

[5] Goodarzi, F., & Zendehboudi, S. (2020). Effects of salt and surfactant on interfacial characteristics of water/oil systems: Molecular dynamic simulations and dissipative particle dynamics. *Industrial and Engineering Chemistry Research*, *58*(20), 8817–8834. https://doi.org/10.1021/acs.iecr.9b00504

[6] Hasanov, E. E., Rahimov, R. A., Abdullayev, Y., & Ahmadova, G. A. (2023). Symmetric and Dissymmetric Pseudo-gemini Amphiphiles Based on Propoxylated Ethyl Piperazine and Fatty Acids. *ChemistrySelect*, *8*(48), e202303942. https://doi.org/10.1002/slct.202303942

[7] Hoogerbrugge, P. J., & Koelman, J. M. V. A. (1992). Simulating microscopic hydrodynamic phenomena with dissipative particle dynamics. *Epl*, *19*(3), 155–160. https://doi.org/10.1209/0295-5075/19/3/001

[8] Espanol, P., & Warren, P. (1995). Statistical mechanics of dissipative particle dynamics. *Epl*, *30*(4), 191–196. https://doi.org/10.1209/0295-5075/30/4/001

[9] Groot, R. D., & Rabone, K. L. (2001). Mesoscopic simulation of cell membrane damage, morphology change and rupture by nonionic surfactants. *Biophysical Journal*, *81*(2), 725–736. https://doi.org/10.1016/S0006-3495(01)75737-2

[10] Groot, R. D., & Warren, P. B. (1997). Dissipative particle dynamics: Bridging the gap between atomistic and mesoscopic simulation. *Journal of Chemical Physics*, *107*(11), 4423–4435. https://doi.org/10.1063/1.474784

[11] Anderson, R. L., Bray, D. J., Del Regno, A., Seaton, M. A., Ferrante, A. S., & Warren, P. B. (2018). Micelle Formation in Alkyl Sulfate Surfactants Using Dissipative Particle Dynamics [Research-article]. *Journal of Chemical Theory and Computation*, *14*(5), 2633–2643. https://doi.org/10.1021/acs.jctc.8b00075

[12] Li, Y., Zhang, H., Bao, M., & Chen, Q. (2012). Aggregation Behavior of Surfactants with Different Molecular Structures in Aqueous Solution: DPD Simulation Study. *Journal of Dispersion Science and Technology*, *33*(10), 1437–1443. https://doi.org/10.1080/01932691.2011.620897

[13] Anderson, R. L., Bray, D. J., Ferrante, A. S., Noro, M. G., Stott, I. P., & Warren, P. B. (2017). Dissipative particle dynamics: Systematic parametrization using water-octanol partition coefficients. *Journal of Chemical Physics*, *147*(9). https://doi.org/10.1063/1.4992111